

pubs.acs.org/acsapm Letter

Oligosiloxane-Based Epoxy Vitrimers: Adaptable Thermosetting Networks with Dual Dynamic Bonds

Amelia A. Putnam-Neeb, Alex Stafford, Sachin Babu, Steven J. Chapman, Christina M. Hemmingsen, Md. Sherajul Islam, Ajit K. Roy, Julia A. Kalow, Vikas Varshney, Dhriti Nepal, and Luke A. Baldwin*



Cite This: https://doi.org/10.1021/acsapm.3c03082



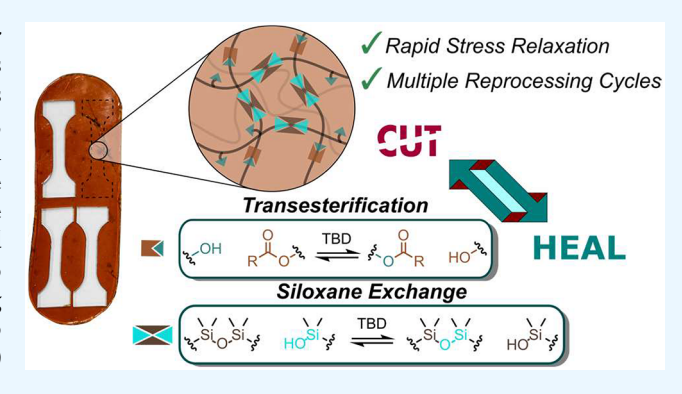
ACCESS

III Metrics & More

Article Recommendations

s Supporting Information

ABSTRACT: Embedding dynamic covalent bonds into polymer compositions transforms static thermosets into active materials with the reprocessability of thermoplastics and the bulk properties of cross-linked networks. This class of next-generation materials, called covalent adaptable networks, shows significant promise in composites, soft optoelectronics, and robotics. Herein, we synthesized two oligosiloxane-based epoxy networks that provide fast dynamic bond exchange. Oligosiloxane diepoxides were cured with stoichiometric amounts of 1,2-phenylenediacetic acid to generate epoxy acid networks with two dynamic covalent bonding mechanisms. The resulting polymer networks provided access to fast stress-relaxation times (1–10 min) at temperatures of only 130 °C with excellent reprocessability.



KEYWORDS: vitrimers, covalent adaptable networks, polymer reprocessing, transesterification, siloxane exchange

ynamic bonds in organic materials are a prominent feature within next-generation materials that help to overcome the limitations in traditional thermosets. Dynamic bonds provide access to functionality that is not possible in irreversible (static) networks. Thermosetting resins, a class of static networks, have excellent stability and mechanical properties as a result of their highly cross-linked 3D architecture and have been utilized in a wide variety of applications including coatings, composites, and robotics.^{1,2} While static networks offer structural and chemical stability ideal for load-bearing structures, these materials lack adaptable functionality. Covalent adaptable networks (CANs), in contrast, are a class of thermosetting polymers with dynamic cross-linking bonds embedded throughout the material (Figure 1). Depending on the exchange mechanism, these networks are often further categorized as dissociative CANs (Diels-Alder reactions being a hallmark example) and associative CANs (often called vitrimers). Some of the more common vitrimerbased bond exchanges include esters, vinylogous urethanes, siloxanes, imines, and acetals.^{3,4} It should be noted, however, that there are many complex network systems with unique properties in these broad categories.^{5,6} These bonds can exchange in the presence of stimuli such as heat or light, which can be utilized for self-healing, welding, reconfiguration, and recycling.^{7,8} These dynamic bonds offer significant functional advantages but may occasionally impact dimensional stability or creep.

Siloxanes have often been used in thermosets and elastomers due to excellent thermal and chemical stability as a result of the high bond strength of the Si-O bond (bond dissociation energy of ~525 kJ·mol⁻¹).¹⁰ To prompt siloxane exchanges and create an adaptable network, strong bases such as tetramethylammonium hydroxide or potassium hydroxide have been added to induce Si-O bond cleavage and the formation of anionic SiO (silanolate) moieties throughout the network. The silanolate groups can then exchange with siloxanes in a substitution-like reaction. These approaches have proved useful in both elastomers¹¹ and thermosets. ^{12,13} Recently, there has been work on direct silyl ether metathesis using catalysts, 14 Bronsted or Lewis acids, or the introduction of free hydroxyls into the network. 10,13 Du Prez and coworkers have developed siloxane-containing vitrimers with very fast dynamics (below 10 s) in the presence of basic catalysts. 15,16 Due to the flexibility of the siloxane units, the prepared resins exhibited low viscosities, which offers significant advantages for fiber-reinforced polymer composite manufacturing. Additionally, it has been shown that the

Special Issue: Early Career Forum 2024

Received: December 16, 2023 Revised: January 26, 2024 Accepted: January 29, 2024

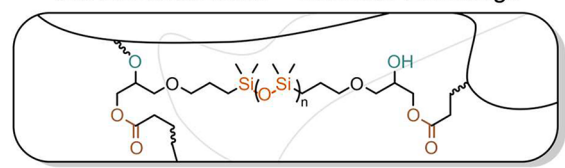


Previous Work:

Transesterification

Current Work:

Transesterification + Siloxane Exchange



✓ Rapid Stress Relaxation: < 1 min. @ 130 °C</p>
✓ Multiple Reprocessing Cycles

Figure 1. Overview of the present work that utilizes dual dynamic bonds catalyzed by the same catalyst to achieve fast stress relaxation and self-healing vitrimers.

incorporation of siloxane groups into reprocessable networks improves the dielectric properties and ductility. ^{17,18}

Although there are a few examples of networks with multiple dynamic bonds in a single network, many of these systems consist of a mix of covalent and noncovalent bonds rather than purely covalent bonds. ¹⁹ In contrast, dual dynamic covalent bond networks are less prevalent but may offer improved properties. With these reports in mind, we sought to embed two active covalent bonds into a single polymer network and explore the resulting material properties. Herein, we describe an oligosiloxane-based adaptable network (Figure 1) with excellent reprocessing characteristics and fast dynamic bond

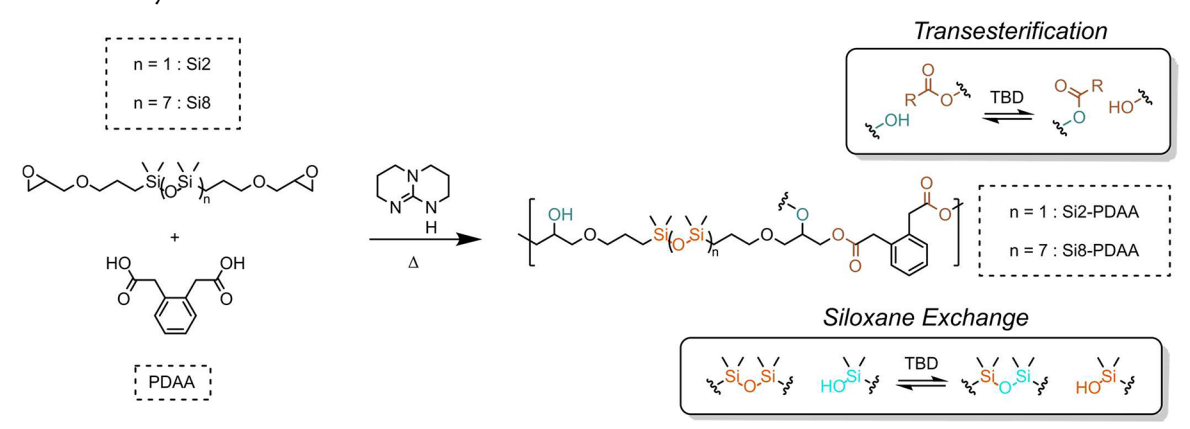
exchanges. This system harnesses 1,5,7-triazabicyclo [4.4.0] dec-5-ene (TBD)-catalyzed transesterification and siloxane exchange mechanisms in a single material to create multifunctional materials with favorable properties.

To obtain a dual dynamic bond exchange network, two diepoxide siloxanes were selected as the diepoxide monomers: a disiloxane (Si2) and an oligosiloxane (Si8), each terminated with glycidyl ether groups (Scheme 1). While prior work has used amine hardeners for similar systems, 15 we instead utilized the dicarboxylic acid 1,2-phenylenediacetic acid (PDAA) to install esters for incorporating two dynamic bonds into one network. We expect the low intrinsic viscosity attained by the siloxane bonds to offer processing advantages and the dual dynamic bonds to impart unique self-healing behavior. For example, the lower viscosity (8-12 mPa·s⁻¹) of our disiloxane diepoxide (Si2) could be beneficial for fiber-reinforced composite manufacturing to better impregnate fibers with vacuum infiltration¹⁷ compared to the common diepoxide cross-linker diglycidyl ether of bisphenol A, which has a viscosity of $11000-16000 \text{ mPa} \cdot \text{s}^{-1}.20$

To synthesize the networks, the siloxane diepoxide (Si2 or Si8) and the dicarboxylic acid components were mixed at a 1:1 stoichiometric ratio of acid/epoxide at 150 °C, at which time TBD was added and the resin was pour-cast into a preheated mold. These elevated temperatures were needed as a result of the high melting temperature of PDAA. After casting, the material was further cured at 150 °C for 14 h. This provided ample time for epoxide consumption and subsequent transesterification reactions to reach equilibrium in the network²¹ (see the Supporting Information, SI). These samples could be cast as individual specimens or laser-cut into the desired shapes for further testing. Si2 and Si8 networks cured with PDAA are termed Si2-PDAA and Si8-PDAA for subsequent discussion.

Both the Si2-PDAA and Si8-PDAA networks showed glass transition temperatures $(T_{\rm g})$ under room temperature, as evidenced by differential scanning calorimetry (DSC) shown in Figures S1–S3. Triplicate experiments provided an average $T_{\rm g}$ of $-18.41~{}^{\circ}{\rm C}$ for Si2-PDAA and $-57.2~{}^{\circ}{\rm C}$ for Si8-PDAA, indicating that a fairly significant reduction in $T_{\rm g}$ can be obtained with rather minimal extension of the siloxane backbone (Table 1). Dynamic mechanical analysis (DMA) experiments (Figures S4–S7) further confirmed these findings with $T_{\rm g}$ values of 11 ${}^{\circ}{\rm C}$ for Si2-PDAA and $-25~{}^{\circ}{\rm C}$ for Si8-PDAA, taken as the peaks of the tan δ curve. The tan δ peak

Scheme 1. General Synthesis of Vitrimers Si2-PDAA and Si8-PDAA



^aThe inset showcases the dynamic covalent bonds catalyzed by TBD.

Table 1. Thermal Characterization of Si2-PDAA and Si8-PDAA

vitrimer	T_{g}^{a} (°C)	$T_{\rm d}^{\ b}$ (°C)	E_a^c (kJ·mol ⁻¹)	$T_{\rm v}^{\ c}$ (°C)
Si2-PDAA	11 ± 1	243	65.7	-12.1
	(-18.41 ± 0.04)		69.5	
Si8-PDAA	-25 ± 2	254	91.6	18.7
	(-57.2 ± 0.2)		95.9	

^aThe values in parentheses are from DSC; those not in parentheses are from DMA. ^b5% weight loss. ^cSee Maxwell model in the SI.

for the Si8-based material was broader than that of the short siloxane chain counterpart (Figure S4). This result typically indicates a less uniform material due to the larger oligosiloxane component, which was supported by a decrease in the crosslink density (ν_c) between the short-chain Si2 (260 mol·m⁻³) and the longer Si8 (120 mol·m⁻³) networks (Table S1). Similarly, the storage modulus of the network in the rubbery regime ($T_{\rm g}$ + 50 °C) decreased from 2.1 MPa for the disiloxane (Si2) to 0.84 MPa for the Si8 material due to the increased siloxane content. The swelling ratios of the vitrimers in CHCl₃, tetrahydrofuran, and toluene (Figures S8 and S9) show a high degree of swelling in CHCl₃ of up to 378% and 444% for Si2-PDAA and Si8-PDAA, respectively. Furthermore, gel contents of 80–90% for the vitrimers indicate satisfactory cross-linking after curing.

Stress-relaxation experiments were performed to document the dynamic behavior of the networks at elevated temperatures (Figures 2 and S10 and S11). The characteristic stress-relaxation time (τ^*) values, defined as the time required for the vitrimer to relax to 1/e of its initial stress, decrease as the temperature is raised from 90 to 130 °C (Figure 2A).

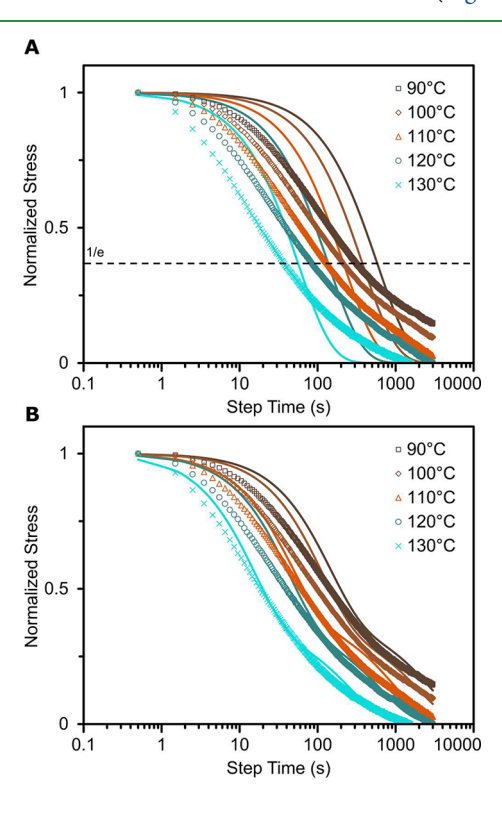


Figure 2. Stress-relaxation curve for Si2-PDAA. The solid lines are predicted traces using (A) one-element and (B) two-element Maxwell models.

Remarkably, Si2-PDAA exhibits a relaxation time of ~40 s at a temperature of only 130 °C. Previously reported higher T_{σ} siloxane-based vitrimers required elevated temperatures (>180 °C) to achieve similar relaxation times. 15,16 This rapid stress relaxation correlates with the low topology freezing transition temperature (T_v) determined from the Arrhenius plot of τ^* (Tables 1 and S12 and S13). This, in conjunction with the low T_{σ} of these materials, leads to accelerated stress relaxation. Previously reported siloxane exchanges often exhibit slower stress-relaxation times because exchange frequently occurs through an S_N2-type mechanism via silanolates and are ratelimited by the nucleophilicity of the generated silanolate. Saed and Terentjev²² also demonstrate this shift in a mechanism with a siloxane-based liquid-crystal elastomer wherein the use of TBD over other bases rapidly improves the stress-relaxation rate. The concerted TBD mechanism¹⁵ in the presence of free hydroxyl groups leads to faster τ^* values. However, τ^* assumes a single-element Maxwell model. Prior work has demonstrated that generalized Maxwell models can better fit complex networks characterized by more than one mechanism or environment for exchange. 23 Therefore, we also fit our data to a two-element Maxwell model, which provided an improved fit for the Si2 relaxation data (Figure 2B). Si8-PDAA data were also fit using the two-element model and demonstrate a similar improved fit (Figure S10). Both two-element models show improved fits, and the resulting $\tau_{\rm A}$ and $\tau_{\rm B}$, separated by about 1 order of magnitude, could be attributed to two independent modes of relaxation, consistent with two unique bond exchanges within the system. When using the two-element Maxwell model, the flow activation energies were calculated for each mode of Si2-PDAA (65.7 and 69.5 kJ·mol⁻¹ for the fast and slow modes, respectively) and Si8-PDAA (91.6 and 95.9 kJ·mol⁻¹) (Table 1). These results align with prior reported TBD-catalyzed siloxane-based vitrimers (~87 kJ·mol⁻¹). 15,16 The slight decrease in the observed E_a for Si2-PDAA may be a result of multiple relaxation modes occurring (siloxane exchanges and transesterification). We can visualize the full distribution of relaxation time scales without making assumptions about the number of modes using a continuous relaxation spectrum, based on an infinite number of Maxwell elements^{24,25} (Figures S14 and S15). Continuous relaxation spectra for Si2-PDAA calculated from the stress relaxation data exhibit two to three independent stress relaxation modes, further supporting the use of a multielement model, whereas relaxation spectra for Si8-PDAA exhibit one dominant relaxation mode (see the SI).

Computational efforts can often provide valuable insight into the inherent reactivity of chemical moieties in dynamic bond exchanges such as TBD-catalyzed transesterification.²⁶ Siloxane exchanges, however, have not been significantly explored computationally. Because our dual dynamic system contains both esters and siloxanes, we performed density functional theory (DFT) computations of the presumed network components to provide additional insights into the siloxane exchange mechanism at work. Simplified versions of siloxane and silanol were optimized at the gas phase using the B3LYP functional²⁷⁻²⁹ with DFT-D3 van der Waals corrections implemented in the NWChem³⁰ to calculate the highest occupied molecular orbital (HOMO) and lowest unoccupied molecular orbital (LUMO) using the 6-31+G(d) basis set^{31,32} (Figure S16). Our calculations assert that the siloxane shows pronounced orbitals in the LUMO and agree with the underlying assumption that it would participate as an

ACS Applied Polymer Materials

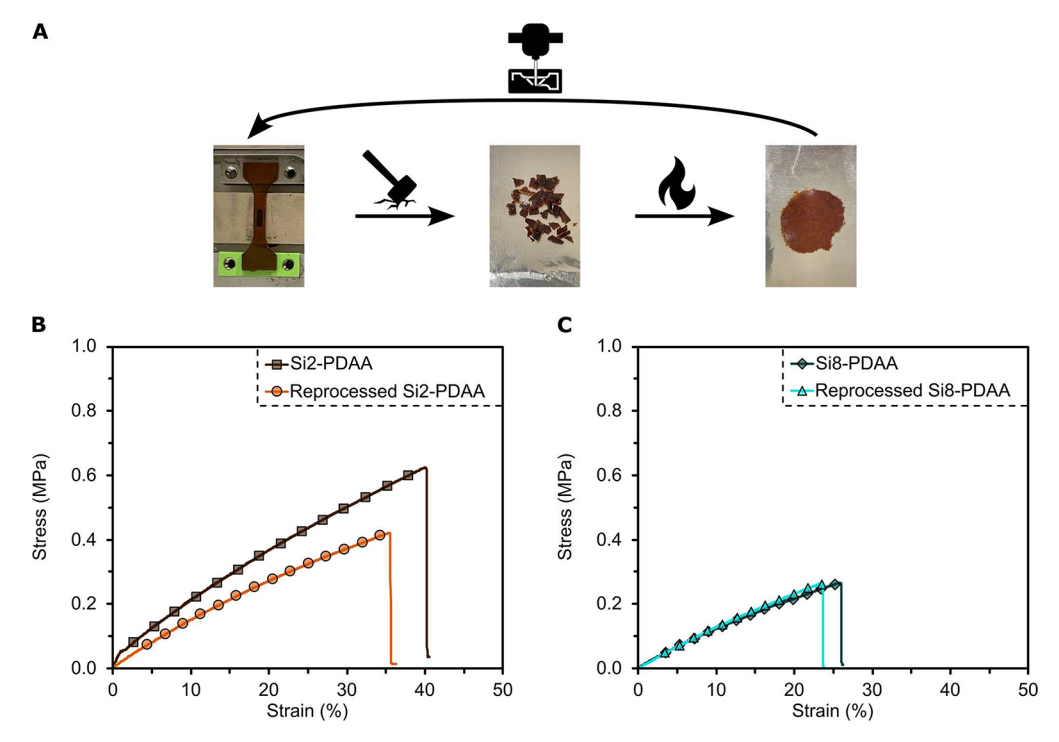


Figure 3. (A) Reprocessing cycle of Si2-PDAA and Si8-PDAA. Dogbones were laser-cut from the sample. The destroyed sample was reprocessed at 150 °C with ~4500 lbs. of force for 45 min. (B) Representative stress—strain curves of Si2-PDAA (brown) and 5× reprocessed Si2-PDAA (orange). (C) Representative stress—strain curves of Si8-PDAA (teal) and 5× reprocessed Si8-PDAA (aqua).

electrophile in the presence of silanol species formed during dynamic bond exchange. These calculations serve to provide additional evidence that multiple covalent moieties are presumably active in the network. While further simulations may be able to shed additional light on the competitive nature of transesterification and siloxane exchange, we also synthesized an analogous single dynamic bond vitrimer based on 1,4butanediol diglycidyl ether (BDDE) and PDAA to analyze the impact of multiple dynamic bonds.³³ The BDDE-PDAA network is imbued with ester linkages but lacks siloxane moieties (Scheme S5), which limits the network to a single class of dynamic bond exchange. This new network exhibited a $T_{\rm g}$ of 18.57 °C (Figure S7) and, upon stress-relaxation experiments at 120 °C, exhibited a stress-relaxation time significantly slower than that of the dual covalent bond system, failing to reach 1/e of its initial stress within 50 min (Figure S11). While some of these characteristic thermomechanical properties are dictated by the chemical network structure, we believe this provides evidence that the siloxane exchange embedded in the dual dynamic bond vitrimer affords accelerated network reorganization.

Tensile testing was also performed to document the mechanical properties of the materials (Figures 3 and S17–S21). Stress—strain experiments provide Young's moduli (E) of 1.7 and 1.29 MPa for the Si2-PDAA and Si8-PDAA networks, respectively (Table 2). The Si2-based network offers slightly better strain at break (40%), ultimate tensile strength (0.5 MPa), and toughness (120 kJ·mol $^{-3}$), which may be a result of the increased cross-link density with the shorter siloxane chain (260 mol·m $^{-3}$) compared to the longer chain Si8 network (120 mol·m $^{-3}$). The single dynamic bond BDDE—PDDA network exhibited a $T_{\rm g}$ of 18.57 °C, a Young's modulus of 1.9 MPa, a tensile strength of 0.67 MPa, and an elongation at break of 52% (Table S2). This is comparable to

Table 2. Mechanical Characterization of the Original and 5× Reprocessed Si2-PDAA and Si8-PDAA

vitrimer	E (MPa)	tensile strength (MPa)	strain at break (%)	toughness (kJ·m ⁻³)
Si2-PDAA	1.7 ± 0.3	0.5 ± 0.1	40 ± 3	120 ± 30
reprocessed Si2-PDAA	1.48 ± 0.04	0.40 ± 0.04	37 ± 6	80 ± 20
Si8-PDAA	1.29 ± 0.07	0.25 ± 0.01	24 ± 2	30 ± 9
reprocessed Si8-PDAA	1.5 ± 0.2	0.30 ± 0.04	24 ± 1	38 ± 5

the properties of the Si2-PDAA vitrimer, which reaffirms that the accelerated stress relaxation of the oligosiloxane-based dual covalent vitrimer stems from the siloxane unit.

Siloxane side chains, exogeneous fillers, and multifunctional cross-linkers can offer a way to further tailor and improve the mechanical properties of these materials.³⁴ To probe this further, we added citric acid (CA), a naturally occurring organic acid, into the network. Prior reports of the enhanced mechanical properties have been documented when supplementing sebacic acid with CA, leading to increased crosslinking as a result of the three carboxylic acid moieties in the structure.³⁴ To test this, CA was added into the adaptable networks such that 40 mol % of all carboxylic acid groups were derived from CA. For the Si2-PDAA network, the Young's modulus increased substantially from 1.7 to 4.4 MPa, while there was a trade-off between the tensile strength and elongation at break (Table S2). For the Si8-PDAA material, the addition of CA improved mechanical properties with an increase in the modulus, tensile strength, and toughness of the material. These results correspond with the increased crosslink density for both Si2-PDAA (from 260 to 480 mol·m⁻³) and Si8-PDAA (from 120 to ~320 mol·m⁻³) upon the addition of CA. While further testing is required to explore the

self-healing efficiency of the networks after the addition of CA, our results show that this method presents a route to modulate the mechanical properties of these networks.

To establish the utility of our oligosiloxane epoxy materials in polymer reprocessing, Si2-PDAA and Si8-PDAA were reprocessed at 150 °C, which is well below the 5% weight loss temperature (T_d) of 243 °C as measured by thermogravimetric analysis (TGA) (Table 1 and Figures S22 and S23). To test the tolerance of these materials to prolonged damage, pristine Si2-PDAA and Si8-PDAA materials were cut into many pieces and reformed in a hot press using ~4500 lbs of force at 150 °C for 45 min. This process was repeated five times successively before retesting the material properties (Figure 3). Tensile tests illustrated superior network stability, as evidenced by the near full retention of the Young's modulus, tensile strength, and strain at break of the original and 5× reprocessed materials (Table 2). Although there are some subtle variations in the mechanical properties of the original and reprocessed samples, we attribute this deviation to nonuniformity within our networks. Unlike defined networks,³⁵ random networks can have a higher propensity to exhibit changes in the chemical cross-links, polymer chain entanglements, and morphology over multiple reprocessing cycles. Comparing the original and reprocessed samples using t-tests, it appears that the majority of the mechanical properties are within variance levels and are not statistically different after reprocessing (Table S3).

In summary, we synthesized oligosiloxane-based epoxy acid vitrimers that provide fast dynamic bond exchange in the presence of TBD. Two oligosiloxane diepoxides were selected and separately cured with stoichiometric amounts of a dicarboxylic acid to generate epoxy vitrimer networks with free hydroxyl groups. The resulting dual dynamic bonds embedded in the system provided fast stress-relaxation times (1-10 min) at temperatures of only 130 °C. While many vitrimers require prolonged heating at elevated temperatures (>200 °C), we have demonstrated that extended reprocessing can be accomplished at 150 °C with excellent retention of the mechanical properties. Overall, this work provides a great framework to utilize epoxy acids and siloxanes, two commonly employed chemical motifs in thermosetting polymers, for dynamic materials. Furthermore, the low viscosity of the siloxane monomers may offer further advantages for composite manufacturing processes.

ASSOCIATED CONTENT

Supporting Information

The Supporting Information is available free of charge at https://pubs.acs.org/doi/10.1021/acsapm.3c03082.

Materials and methods, synthesis, equipment and instrumentation, and material characterization (PDF)

AUTHOR INFORMATION

Corresponding Author

Luke A. Baldwin — Air Force Research Laboratory, Wright Patterson Air Force Base, Dayton, Ohio 45433, United States; orcid.org/0000-0002-7787-238X; Email: luke.baldwin.1@us.af.mil

Authors

Amelia A. Putnam-Neeb — Air Force Research Laboratory, Wright Patterson Air Force Base, Dayton, Ohio 45433, United States; oorcid.org/0000-0003-0048-2786

Alex Stafford – Air Force Research Laboratory, Wright Patterson Air Force Base, Dayton, Ohio 45433, United States; UES, Inc., Dayton, Ohio 45432, United States

Sachin Babu — Air Force Research Laboratory, Wright Patterson Air Force Base, Dayton, Ohio 45433, United States; UES, Inc., Dayton, Ohio 45432, United States

Steven J. Chapman – Department of Chemistry, Northwestern University, Evanston, Illinois 60208, United States; orcid.org/0000-0003-1570-4580

Christina M. Hemmingsen – Department of Chemistry, Northwestern University, Evanston, Illinois 60208, United States; © orcid.org/0000-0002-6384-6420

Md. Sherajul Islam — Spectral Energies, LLC, Dayton, Ohio 45430, United States

Ajit K. Roy — Air Force Research Laboratory, Wright
Patterson Air Force Base, Dayton, Ohio 45433, United States
Julia A. Kalow — Department of Chemistry, Northwestern
University, Evanston, Illinois 60208, United States;
orcid.org/0000-0002-4449-9566

Vikas Varshney — Air Force Research Laboratory, Wright Patterson Air Force Base, Dayton, Ohio 45433, United States; © orcid.org/0000-0002-2613-458X

Dhriti Nepal — Air Force Research Laboratory, Wright Patterson Air Force Base, Dayton, Ohio 45433, United States; Occid.org/0000-0002-0972-9960

Complete contact information is available at: https://pubs.acs.org/10.1021/acsapm.3c03082

Author Contributions

A.A.P.-N. and L.A.B.: conceptualization. A.A.P.-N., S.B., S.J.C., C.M.H., M.S.I., J.A.K., A.K.R., D.N., and L.A.B.: methodology. A.A.P.-N., S.B., A.S., S.J.C., C.M.H., and M.S.I.: investigation. A.A.P.-N., S.B., A.S., and L.A.B.: visualization. J.A.K. and L.A.B.: funding acquisition. L.A.B.: project administration. J.A.K. and L.A.B.:supervision. A.A.P.-N., A.S., and L.A.B.: writing the original draft. The final manuscript was written through contributions of all authors. All authors have given approval to the final version of the manuscript.

Funding

This research was funded through support by the Air Force Research Laboratory, Materials and Manufacturing Directorate, as well as the Air Force Office of Scientific Research under Grant 22RXCOR014. J.A.K. was supported by the Center for the Chemistry of Molecularly Optimized Networks, National Science Foundation, under Grant CHE-2116298.

Notes

The authors declare no competing financial interest.

ACKNOWLEDGMENTS

This research was performed while A.A.P.-N. held a National Research Council Research Associateship award at the Air Force Research Laboratory. S.J.C. acknowledges support from the Arnold and Mabel Beckman Foundation with a postdoctoral fellowship in the chemical sciences. C.M.H. acknowledges support from the National Science Foundation Graduate Research Fellowship under Grant DGE-2234667.

ABBREVIATIONS

CA, citric acid; CANs, covalent adaptable networks; DMA, dynamic mechanical analysis; DSC, differential scanning calorimetry; PDAA, 1,2-phenylenediacetic acid; TBD, 1,5,7-triazabicyclo[4.4.0]dec-5-ene; TGA, thermogravimetric analysis

REFERENCES

- (1) Kausar, A. Role of Thermosetting Polymer in Structural Composite. Am. J. Polym. Sci. Eng. 2017, 5, 1–12.
- (2) Morici, E.; Dintcheva, N. Recycling of Thermoset Materials and Thermoset-Based Composites: Challenge and Opportunity. *Polymers* **2022**, *14* (9), 4153–4164.
- (3) Schenk, V.; Labastie, K.; Destarac, M.; Olivier, P.; Guerre, M. Vitrimer composites: current status and future challenges. *Materials Advances* **2022**, 3 (22), 8012–8029.
- (4) Podgorski, M.; Fairbanks, B.; Kirkpatrick, B.; McBride, M.; Martinez, A.; Dobson, A.; Bongiardina, N. J.; Bowman, C. N. Toward Stimuli-Responsive Dynamic Thermosets through Continuous Development and Improvements in Covalent Adaptable Networks (CANs). *Adv. Mater.* **2020**, 32 (20), No. 1906876.
- (5) Herbert, K. M.; Getty, P. T.; Dolinski, N. D.; Hertzog, J. E.; de Jong, D.; Lettow, J. H.; Romulus, J.; Onorato, J. W.; Foster, E. M.; Rowan, S. J. Dynamic reaction-induced phase separation in tunable, adaptive covalent networks. *Chem. Sci.* **2020**, *11* (19), 5028–5036.
- (6) Dodo, O. J.; Raji, I. O.; Arny, I. J.; Myers, C. P.; Petit, L.; Walpita, K.; Dunn, D.; Thrasher, C. J.; Konkolewicz, D. Dynamic polymer nanocomposites towards strain sensors and customizable resistors. *RSC Applied Polymers* **2023**, *1*, 30–45.
- (7) Shi, Q.; Jin, C.; Chen, Z.; An, L.; Wang, T. On the Welding of Vitrimers: Chemistry, Mechanics and Applications. *Adv. Funct. Mater.* **2023**, 33 (36), No. 2300288.
- (8) Jia, Y.; Ling, F.; Qian, J.; Chen, Q.; Zhao, Z.; Li, Y. Fast Damage-Healing of Rigid Photocuring 3D Printing Materials Capable of Directly Recycling in 3D Printing. ACS Macro Lett. 2023, 12 (6), 719–724.
- (9) Van Lijsebetten, F.; Debsharma, T.; Winne, J. M.; Du Prez, F. E. A Highly Dynamic Covalent Polymer Network without Creep: Mission Impossible? *Angew. Chem., Int. Ed.* **2022**, *61* (48), No. e202210405.
- (10) Tretbar, C. A.; Neal, J. A.; Guan, Z. Direct Silyl Ether Metathesis for Vitrimers with Exceptional Thermal Stability. *J. Am. Chem. Soc.* **2019**, *141* (42), 16595–16599.
- (11) Saed, M. O.; Terentjev, E. M. Siloxane crosslinks with dynamic bond exchange enable shape programming in liquid-crystalline elastomers. *Sci. Rep.* **2020**, *10* (1), No. 6609.
- (12) Putnam-Neeb, A. A.; Kaiser, J. M.; Hubbard, A. M.; Street, D. P.; Dickerson, M. B.; Nepal, D.; Baldwin, L. A. Self-healing and polymer welding of soft and stiff epoxy thermosets via silanolates. *Adv. Compos. Hybrid Mater.* **2022**, *5*, 3068–3080.
- (13) Ma, J.; Porath, L. E.; Haque, M. F.; Sett, S.; Rabbi, K. F.; Nam, S.; Miljkovic, N.; Evans, C. M. Ultra-thin self-healing vitrimer coatings for durable hydrophobicity. *Nat. Commun.* **2021**, *12* (1), No. 5210.
- (14) Juraskova, A.; Olsen, S. M.; Skov, A. L. Reversible Dynamic Behavior of Condensation-Cured Silicone Elastomers Caused by a Catalyst. *Macromol. Mater. Eng.* **2023**, *308* (6), No. 2200615.
- (15) Debsharma, T.; Amfilochiou, V.; Wroblewska, A. A.; De Baere, I.; Van Paepegem, W.; Du Prez, F. E. Fast Dynamic Siloxane Exchange Mechanism for Reshapable Vitrimer Composites. *J. Am. Chem. Soc.* **2022**, 144 (27), 12280–12289.
- (16) Debsharma, T.; Engelen, S.; De Baere, I.; Van Paepegem, W.; Du Prez, F. Resorcinol-Derived Vitrimers and Their Flax Fiber-Reinforced Composites Based on Fast Siloxane Exchange. *Macromol. Rapid Commun.* **2023**, 44 (8), No. 2300020.
- (17) Chen, M.; Luo, W.; Lin, S.; Zheng, B.; Zhang, H. Recyclable, reprocessable, self-healing elastomer-like eopoxy vitrimer with low dielectric permittivity and its closed-loop recyclable carbon fiber reinforced composite. *Composites Part B* **2023**, 257, No. 110666.

- (18) Chen, M.; Chen, B.; Li, D.; Luo, W.; Zhang, H. Development of a Multistimulus Response Silicon-Bridged/Fe₃O₄ Epoxy Vitrimer: Controllable Welding, Crack Healing, and Shape Memory. *ACS Appl. Polym. Mater.* **2023**, 5 (12), 9931–9939.
- (19) Zhou, L.; Zhou, L.; Chen, R.; Chang, G.; Zhang, K.; Chen, M. Coded Interlocked Covalent Adaptable Networks Enabled by Parallel Connections of Cation— π Interactions and Aromatic Disulfide Bonds in Epoxy. ACS Applied Polymer Materials 2023, 5 (10), 8442–8449.
- (20) Malburet, S.; Bertrand, H.; Richard, C.; Lacabanne, C.; Dantras, E.; Graillot, A. Biobased Epoxy Reactive Diluents Prepared from Monophenol Derivatives: Effect on Viscosity and Glass Transition Temperature of Epoxy Resins. *RSC Adv.* **2023**, *13* (22), 15099–15106.
- (21) Bakkali-Hassani, C.; Edera, P.; Langenbach, J.; Poutrel, Q. A.; Norvez, S.; Gresil, M.; Tournilhac, F. Epoxy Vitrimer Materials by Lipase-Catalyzed Network Formation and Exchange Reactions. *ACS Macro Lett.* **2023**, *12* (3), 338–343.
- (22) Saed, M. O.; Terentjev, E. M. Catalytic Control of Plastic Flow in Siloxane-Based Liquid Crystalline Elastomer Networks. *ACS Macro Lett.* **2020**, *9* (5), 749–755.
- (23) El-Zaatari, B. M.; Ishibashi, J. S. A.; Kalow, J. A. Cross-linker control of vitrimer flow. *Polym. Chem.* **2020**, *11* (33), 5339–5345.
- (24) Grindy, S. C.; Learsch, R.; Mozhdehi, D.; Cheng, J.; Barrett, D. G.; Guan, Z.; Messersmith, P. B.; Holten-Andersen, N. Control of hierarchical polymer mechanics with bioinspired metal-coordination dynamics. *Nat. Mater.* **2015**, *14*, 1210–1216.
- (25) Shanbhag, S. pyReSpect: A Computer Program to Extract Discrete and Continuous Spectra from Stress Relaxation Experiments. *Macromol. Theory Simul.* **2019**, 28 (3), No. 1900005.
- (26) Bhusal, S.; Oh, C.; Kang, Y.; Varshney, V.; Ren, Y.; Nepal, D.; Roy, A.; Kedziora, G. Transesterification in vitrimer polymers using bifunctional catalysts: Modeled with solution-phase experimental rates and theoretical analysis of efficiency and mechanisms. *J. Phys. Chem. B* **2021**, *125* (9), 2411–2424.
- (27) Kim, K.; Jordan, K. D. Comparison of Density Functional and MP2 Calculations on the Water Monomer and Dimer. *J. Phys. Chem.* **1994**, 98 (40), 10089–10094.
- (28) Stephens, P. J.; Devlin, F. J.; Chabalowski, C. F.; Frisch, M. J. Ab Initio Calculation of Vibrational Absorption and Circular Dichroism Spectra Using Density Functional Force Fields. *J. Phys. Chem.* **1994**, 98 (45), 11623–11627.
- (29) Cramer, C. J. Essentials of Computational Chemistry: Theories and Models, 2nd ed.; Wiley, 2004.
- (30) Valiev, M.; Bylaska, E. J.; Govind, N.; Kowalski, K.; Straatsma, T. P.; van Dam, H. J. J.; Wang, D.; Nieplocha, J.; Apra, E.; Windus, T. L.; de Jong, W. A. NWChem: a comprehensive and scalable open-source solution for large scale molecular simulations. *Comput. Phys. Commun.* **2010**, *181*, 1477.
- (31) Clark, T.; Chandrasekhar, J.; Spitznagel, G. W.; Schleyer, P. V. R. Efficient Diffuse Function-Augmented Basis Sets for Anion Calculations. III. The 3-21 G Basis Set for First-Row Elements, Li-F. J. Comput. Chem. 1983, 4, 294–301.
- (32) Frisch, M. J.; Pople, J. A.; Binkley, J. S. Self-consistent Molecular Orbital Methods 25. Supplementary Functions for Gaussian Basis Sets. *J. Chem. Phys.* **1984**, *80*, 3265–3269.
- (33) Huang, X.; Wang, Y.; Ding, C.; Zhang, S.; Duan, X.; Ji, H.; Cai, J.; Wang, Z. High-Performance Epoxy Vitrimers with the Joint Action of Dual Dynamic Covalent Bonds. *ACS Appl. Polym. Mater.* **2024**, *6*, 126–140.
- (34) Altuna, F. I.; Hoppe, C. E.; Williams, R. J. J. Shape memory epoxy vitrimers based on DGEBA crosslinked with dicarboxylic acids and their blends with citric acid. *RSC Adv.* **2016**, *6* (91), 88647–88655.
- (35) Luo, J.; Zhao, X.; Ju, H.; Chen, X.; Zhao, S.; Demchuk, Z.; Li, B.; Bocharova, V.; Carrillo, J.-M. Y.; Keum, J. K.; Xu, S.; Sokolov, A. P.; Chen, J.; Cao, P. Highly Recyclable and Tough Elasticd Vitrimers from a Defined Polydimethylsiloxane Network. *Angew. Chem., Int. Ed.* **2023**, *62* (47), No. e202310989.